REGULAR ARTICLE

blood advances

Characterization and statistical modeling of glycosylation changes in sickle cell disease

Heather E. Ashwood,[1] Christopher Ashwood,[2] Anna P. Schmidt,[1] Rebekah L. Gundry,[2,3] Karin M. Hoffmeister,[1,2] and Waseem Q. Anani[4,5]

[1]Versiti Blood Research Institute, Translational Glycomics Center, Milwaukee, WI; [2]Department of Biochemistry, [3]Center for Biomedical Mass Spectrometry Research, and [4]Department of Pathology, Medical College of Wisconsin, Milwaukee, WI; and [5]Versiti Medical Sciences Institute, Milwaukee, WI

Key Points

- Glycosylation changes on red blood cells and in plasma have been correlated to sickle cell disease and sickle cell trait.
- Samples were analyzed with lectin and glycan microarrays, allowing for rapid screening, but requiring increased computational scrutiny.

Sickle cell disease is an inherited genetic disorder that causes anemia, pain crises, organ infarction, and infections in 13 million people worldwide. Previous studies have revealed changes in sialic acid levels associated with red blood cell sickling and showed that stressed red blood cells bare surface-exposed clustered terminal mannose structures mediating hemolysis, but detailed glycan structures and anti-glycan antibodies in sickle cell disease remain understudied. Here, we compiled results obtained through lectin arrays, glycan arrays, and mass spectrometry to interrogate red blood cell glycoproteins and glycan-binding proteins found in the plasma of healthy individuals and patients with sickle cell disease and sickle cell trait. Lectin arrays and mass spectrometry revealed an increase in α2,6 sialylation and a decrease in α2,3 sialylation and blood group antigens displayed on red blood cells. Increased binding of proteins to immunogenic asialo and sialyl core 1, Lewis A, and Lewis Y structures was observed in plasma from patients with sickle cell disease, suggesting a heightened anti-glycan immune response. Data modeling affirmed glycan expression and plasma protein binding changes in sickle cell disease but additionally revealed further changes in ABO blood group expression. Our data provide detailed insights into glycan changes associated with sickle cell disease and refer glycans as potential therapeutic targets.

Introduction

Sickle cell disease (SCD), the most common hemoglobinopathy, affects up to 100 000 people in the United States and 13 million people worldwide.[1] The inheritance of a homozygous mutation from valine to glutamic acid in the hemoglobin HbS β chain causes polymerization of deoxy sickle hemoglobin within red blood cells (RBCs).[2] In an oxygen-deprived state, RBCs take on a sickled shape and occlude blood vessels. Individuals are afflicted with anemia, pain crises, organ infarction, and infections; however, clinical phenotypes vary and remain unpredictable. Additionally, a heterozygous mutation results in the sickle cell trait (SCT), with predominantly silent features.[3]

SCD requires a multifaceted approach for long-term treatment.[4,5] Current SCD therapies remain limited, usually comprising hydroxyurea therapy,[6] and increasingly gene therapy and stem cell transplants to correct hemoglobin mutations.[7,8] However, the repertoire of potential therapeutic targets continues to grow.[9-11] For example, rivipansel, a glycomimetic pan selectin antagonist, which targeted E-selectin, showed reduced resolution times of vaso-occlusive episodes[12] but ultimately failed to meet its treatment goals.[13]

Submitted 9 September 2020; accepted 20 January 2021; published online 5 March 2021. DOI 10.1182/bloodadvances.2020003376.

The data have been publicly deposited at Glycopost (https://glycopost.glycosmos.org/preview/15566942915f39ca7bd7b83, PIN: 6982) and Panorama Public (https://panoramaweb.org/RBCSickleGlycomics.url). For information, please contact the corresponding author Karin M. Hoffmeister (khoffmeister@versiti.org).

The full-text version of this article contains a data supplement.

Glycans (carbohydrates), biologically diverse cell surface molecules,[14] are often overlooked as potential mediators of vaso-occlusive crises in SCD.[15] Sialic acid (SA; the ultimate "do not eat me" signal) containing glycan motifs on both *N*- and *O*-linked glycans contributes to diverse aspects of immunity, cell–cell interactions, and cell signaling.[16] For example, siglecs drive B-cell development and humoral response using sialyl-glycan recognition by their receptors to modulate immune response.[17,18] Another sialyl-glycan motif, sialyl-Lewis X, binds selectins and promotes leukocyte trafficking to lymph nodes and sites of inflammation.[19,20]

Changes in sialylation and fucosylation are well documented in chronic inflammation.[21,22] Although changes in SA levels are associated with RBC sickling, there are conflicting reports of decreased[23] and increased[24,25] sialylation compared with healthy individuals. This aberrant glycan clustering and exposure of cryptic antigens and new epitopes in sickling RBCs results in antibody formation and cell destruction.[26-28] For example, the anti-Galili (galactose-α-1,3-galactose [α-Gal]) immunoglobulin G (IgG) is increased in SCD, promoting macrophage phagocytosis of sickled RBCs.[29] Although the inflammatory milieu in SCD is expected to increase antibody formation globally,[30,31] little is known with regard to specific glycan motifs and resultant antibodies present in this disease.

To address this knowledge gap and identify potential new therapeutic targets, we analyzed plasma and RBCs using a combination of lectin and glycan microarrays and mass spectrometry and integrated this glycan and antibody data using statistical modeling. Our data show that SCD RBCs have the following: (1) increased α2,6 sialylation; (2) decreased α2,3 sialylation and blood group antigen expression; and (3) increased glycan binding by plasma proteins in SCD to immunogenic asialo and sialyl core 1, Lewis A, and Lewis Y structures, suggesting a heightened anti-glycan immune response. Computational modeling (MixOmics) affirms changes in glycan expression and glycan-binding protein (GBP) binding, including immunoglobulins, of immunogenic glycan structures in SCD, but reveals additional changes, including ABO blood group expression.

Methods

Sample collection and demographics

Whole blood was prospectively obtained with an institutional review board–approved protocol as deidentified residual samples.

Data were collected from a total 50 blood group O and 37 group A African Americans with demographics distributed as in Table 1. SCT samples were collected from donors positive by SICKLEDEX (Somagen Diagnostics, Edmonton, Canada).[32] Hemoglobin levels were between 12.5 and 20.0 g/dL for healthy and SCT samples as per guidelines of blood donation (see https://www.accessdata.fda.gov/scripts/cdrh/cfdocs/cfcfr/cfrsearch.cfm?fr=630.10). SCD samples were acquired before transfusion, and hemoglobin levels were between 0.8 and 2.0 g/dL determined using a Sysmex 2000v. Samples were separated and run based on blood group and disease state, as previous research concluded that sex was not a significant contributor to differential glycosylation.[33]

Whole blood was collected in EDTA and separated by centrifugation (3500*g*, 10 minutes) to remove plasma. All whole blood samples were processed 7 days after collection. Based on previous validation, this allowed for uniformity of sample age without significant loss in glycosylation (supplemental Table 1). Plasma was further centrifuged to remove residual RBC cells and fibrinogen (10 000 rpm, 20 minutes) and stored at −20°C.

Table 1. Patient demographics for samples analyzed

	Group O				Group A			
	Control	SCT	SCD	Total	Control	SCT	SCD	Total
Total	20	10	20	50	20	8	9	37
Sex								
Female	14	2	9	25	8	2	7	17
Male	6	8	11	25	12	6	2	20
Age, y								
15-24	3	4	1	8	2	4	1	7
25-44	6	3	12	21	9	3	5	17
45-64	9	3	7	19	6	0	3	9
65+	2	0	0	2	3	1	0	4
Average age, y	45	32	40	41	45	30	39	40

RBC preparation

The RBC fraction was further processed using a Ficoll-Paque (GE Healthcare) separation and a dextran gradient to purify erythrocytes.[34] Six percent dextran was mixed (1 part) with 1 part RBCs and 2 parts Dulbecco's phosphate-buffered saline (PBS; Gibco/Thermo Fisher Scientific). Erythrocytes were allowed to sediment at room temperature for 15 minutes. The supernatant was removed, and RBC ghosts were obtained as described in Anani et al.[33,35] Patient HbS cells were morphologically counted using a Sysmex 2000v to guarantee a population of 60% or greater.

RBC sample preparation for lectin arrays

To reduce nonspecific binding, lipids were removed from RBCs with a triton extraction buffer.[36] Extraction buffer (500 μL) was added to the RBC pellet, incubated at 4°C with rotation (30 minutes), and centrifuged (16 000*g*, 15 minutes at 4°C), and supernatant collected for analysis.

Protein quantification was performed, and 0.125 μg/mL labeled protein was incubated on a GlycoTechnica LecChip microarray as previously described in Anani et al.[33] The array was scanned at 532 nm with a GlycoStation 2200 (GlycoTechnica), and fluorescence values were analyzed using SignalCapture 3.0 and GlycoStationToolsPro 3.0 (GlycoTechnica).

Plasma sample preparation for glycan arrays

The RayBiotech label-based protocol (https://www.raybiotech.com/glycan-array-100/) for whole plasma was followed. Plasma was diluted 1:4 in Dulbecco's PBS and dialyzed for 3 hours in PBS at 4°C before samples (35 μL) were biotin labeled. RayBiotech Glycan Array 100 slides were blocked for 30 minutes before 80 μg/mL sample was incubated on the arrays with agitation for 2 hours. After washing, the array was dried by centrifugation (1000 rpm, 3 minutes) and scanned in a GenePix 4000B microarray reader (Molecular Devices). Glycan arrays were scanned at 532 nm (450 photomultiplier tubes [PMT], 30% power), and spots were selected using GenePixPro 3.0 software. The median sample-specific

background subtracted data for each glycan was achieved by averaging the 3 highest replicate fluorescent spot values.

Mass spectrometry of RBCs

Sample preparation for glycan analysis. Lipid extracted RBCs were prepared for mass spectrometry from erythrocyte ghosts, as prepared above. Proteins were reduced with 5 mM final concentration of tris(2-carboxyethyl) phosphine at 37°C for 45 minutes and alkylated with a 10 mM final concentration of iodoacetamide for 45 minutes in the dark at room temperature, followed by Qubit analysis for protein quantitation (Thermo Fisher Scientific).

N- and O-glycan release. Protein (25 μg) was immobilized on a polyvinylidene difluoride membrane with subsequent *N*- and *O*-glycan release as previously described.[37,38] Membrane spots were excised and washed in wells of a flat bottom polypropylene 96-well plate. *N*-glycans were released from the membrane-bound protein using 2 U PNGase F (Promega) with overnight incubation (37°C). Following *N*-glycan removal, 500 mM $NaBH_4$ in a 50 mM KOH solution was added to the membrane spots for 16 hours to release reduced *O*-linked glycans by reductive β-elimination. Released *N*-glycans were reduced (1 M $NaBH_4$ in 50 mM KOH solution) for 3 hours (50°C), after which the reaction was neutralized with equimolar glacial acetic acid. Both *N*- and *O*-glycans were desalted and enriched offline using strong cation exchange resin (Dowex 50WX8 [200-400 mesh], Millipore Sigma) followed by porous graphitic carbon (PGC) solid phase extraction micro-columns (Thermo Fisher Scientific).

N- and O-glycan data acquisition. Samples were dissolved in 65 μL of 10 mM NH_4HCO_3 containing 1 μL of dextran ladder internal standard (26 ng, centrifuged to remove particulates),[39] and then 60 μL of resulting solution was transferred to autosampler vials. Samples were randomized before injection. An internal standard-only sample was analyzed between each replicate block to verify no carryover. PGC-liquid chromatography-electrospray ionization- mass spectrometry/mass spectrometry (PGC-LC-ESI-MS/MS) experiments were performed using a nanoLC-2D high-performance liquid chromatography system (Eksigent) interfaced with an LTQ Orbitrap Velos mass spectrometer (Thermo Fisher Scientific). Glycans were separated on a PGC-LC column (3 μm, 100 mm × 0.18 mm, Hypercarb, Thermo Fisher Scientific) maintained at 80°C for *N*-glycans and 40°C for *O*-glycans. To enhance ionization and improve detection of low intensity glycans, postcolumn make-up flow consisting of 100% methanol was used.

Glycan data analysis and library construction. Normalized retention time by dextran ladder was determined as described previously using Skyline, and proprietary raw files were converted to an open and vendor neutral file format, mzML, using Proteowizard v3.0.8725.[39,40] MS2 scans, required for confirmation of glycan composition and structure, were filtered to include only precursor masses consistent with probable human glycan compositions (searched within 20-ppm error with GlycoMod).[41,42]

Glycan quantitation. Skyline v4.2.1.19095 was used for all glycan analysis as we previously described,[37,43] and 99.999% of the isotopic envelope with a centroid mass accuracy value of 20 ppm was used for peak integration for glycan structure measurements. Peak picking was largely automated based on explicit retention time, and integration bounds were manually supervised. Peak areas for each measured glycan structure were exported and normalized to relative signal in Microsoft Excel. Glycan structure relative signal was calculated for the specific glycan structure's peak area as a percentage of the total peak area for all glycan structures measured for each sample.

Glycan structure assignment. MS2 scans were assigned glycan structures based on the existence of A-, B-, C-, X-, Y-, and Z-product ions matched using GlycoWorkBench v2.1 (available from https://code.google.com/archive/p/glycoworkbench/, maximum of 3 glycosidic cleavages and 1 cross-ring cleavage with 0.6-Da mass accuracy).[44] For all MS/MS scans, at least 2 probable glycan structures were used for comparative annotation to assign the most suitable structure assignment. Diagnostic ions were used to confirm glycan motifs as described previously.[42,45] To promote utility of the glycan structure libraries generated here and to adhere to MIRAGE guidelines,[46,47] all data and metadata are available on Glycopost (https://glycopost.glycosmos.org/preview/15566942915f39ca7bd7b83, PIN: 6982)[48] and Panorama Public (https://panoramaweb.org/RBCSickleGlycomics.url).[49]

Data analysis

Array fluorescence data were statistically analyzed as described in Anani et al.[33] Additional details are included in supplemental Methods.

Data Integration Analysis for Biomarker discovery using Latent variable approaches for 'Omics studies (MixOmics or DIABLO) creates pathway linkages between apparently disparate datasets to find correlated probes.[50,51] Data from the same RBC and plasma samples analyzed using lectin and glycan arrays were loaded as individual blocks, normalized as above, and annotated as healthy, SCT, or SCD. The weighted correlations were set to 0.1 between RBC lectin (RBCs analyzed with the lectin array) and plasma glycan (plasma analyzed with the glycan array) data with the remaining associations set to 0. Performance of the data were run with the following parameters: seed 123, Mfold cross-validation, 5 folds, 10 components, and 1000 repeats. The performance was modeled as centroids, mahalanobis, and maximum distances.[52] The smallest overall error rate was selected to choose the most influential probes in distinguishing between cohorts. Probe selection (tuning) was run with the following parameters: seed 123, Mfold cross-validation, 5 folds, 5 components, centroids distance, and 1000 repeats. Once the appropriate dimensions of data and probes were selected, the data were visualized by heat map.

Results

Lectin microarray reveals increased α2,6-sialylation and decreased blood group related lectin binding in SCD RBC glycoproteins

Lectins are typically used for cell typing, histochemical staining, and glycoprotein fractionation.[53] Immobilized lectins on microarrays can rapidly screen samples for glycan changes by comparing differences in expression.[54] We used GlycoTechnica lectin arrays, containing 45 diverse lectins, to determine glycan changes in RBC glycoprotein structures between healthy donors, SCT donors, and SCD patients (Figure 1A). Using sparse partial least squares discriminant analysis (sPLS-DA), lectin binding combinations unique to each cohort were calculated and visualized with a prediction map (Figure 1B). With 1 exception, healthy and SCD

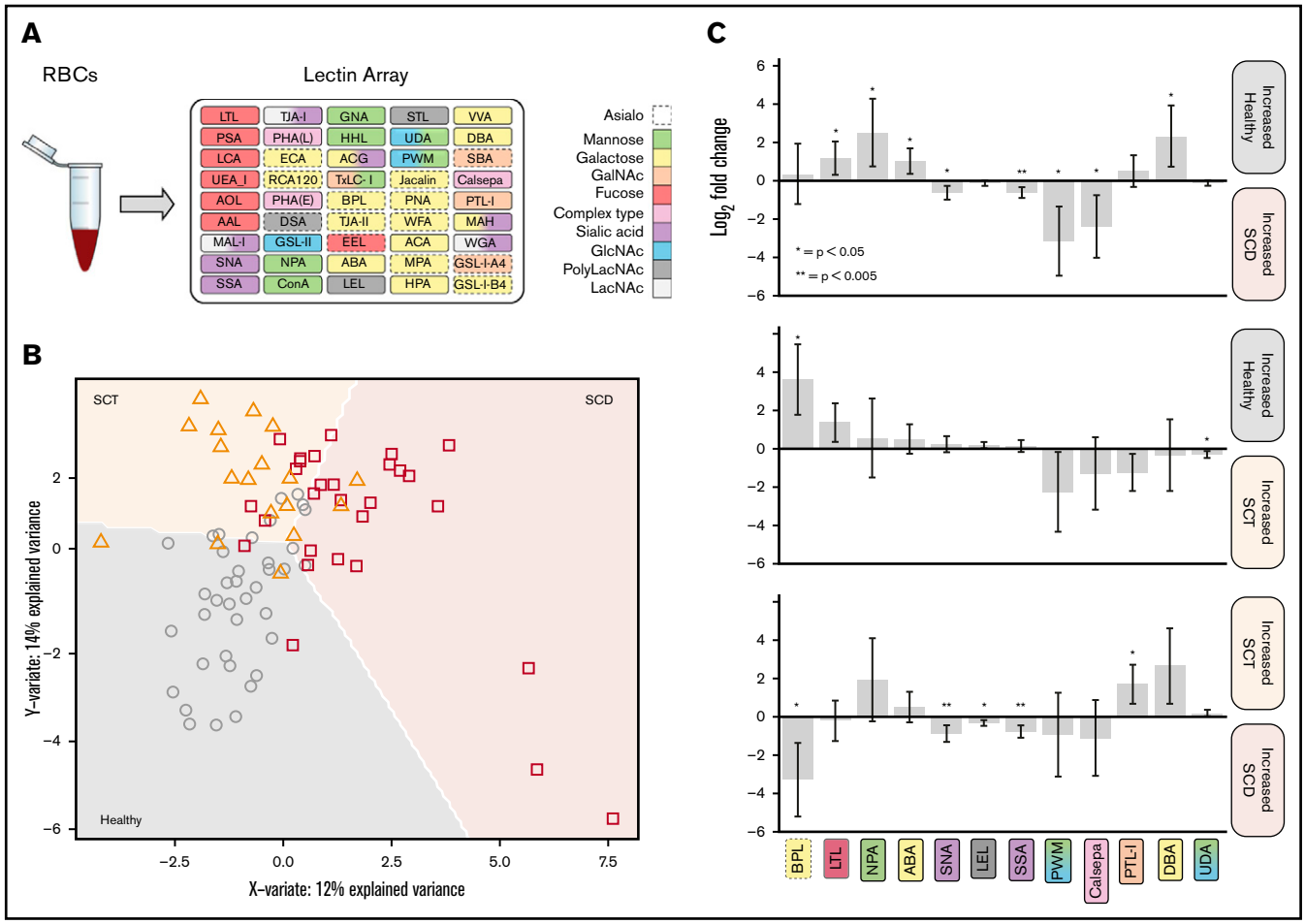

Figure 1. Separation of healthy, SCT, and SCD RBC samples based on lectin specificity of microarrays. (A) RBC samples (ghost cells) were applied to a lectin array (GlycoTechnica) and trends interpreted from fluorescence data. Lectins are colored based in binding specificity (for full specificities see supplemental Table 2). (B) Data were analyzed using the centroids distance method and separated based on disease state (component contributions are listed in supplemental Figure 1). Background shading represents the 95% confidence interval (CI). Receiver operating characteristic values are as follows: Healthy vs all = 0.8046; SCT vs all = 0.6153; SCD vs all = 0.9206. (C) Data normalized using a quantile method and with *t* test statistics performed showed a number of significant changes ($P \leq .05$) in lectin binding between all sample types (95% CI bars shown; for full *t* test results, see supplemental Table 3). Lectin specificities and disease state preferences for each lectin are indicated.

samples were separated easily from one another, whereas the SCT cohort expressed glycan moieties observed in both healthy and SCD groups, precluding a complete separation from both (see supplemental Figure 1 for all lectin contributions).

Pairwise moderated *t* tests identified significant changes in lectin binding between groups (Figure 1C). Healthy donors expressed more terminal fucose (LTL), mannose (NPA), and galactose (ABA and DBA) motifs compared with SCD patients. LTL (blood group O), DBA (blood group A_1), and NPA identify with blood group expression,[33] indicating blood group loss in SCD RBCs. SCD patients expressed more α2,6 SA moieties (SNA, SSA), in addition to terminal GalNAc (PTL-I) and complex bisecting *N*-linked glycans (Calsepa) compared with healthy donors. Healthy and SCT donors differed by increased expression of asialo-galactose (BPL) and terminal mannose/GalNAc (UDA). The statistically significant differences between SCT and SCD included increased terminal GalNAc (PTL-I) and decreased α2,6-sialylation and polylactosamine in SCT.

Mass spectrometry confirms increased α2,6 and reveals decreased α2,3 sialic acid on SCD RBC glycoproteins

To fully assign a structure to a glycan, a combination of MS, biosynthetic rules, chemical and enzymatic treatment, and retention time is necessary.[48] Healthy and SCD RBCs (3 samples each, both blood group O) were analyzed by PGC-LC-MS to define glycan structures. From the mixture of *N*-glycans released from RBCs, 118 structures were quantified over 3 orders of magnitude. These glycans cover all major glycan classes with no clear relationship between class and relative signal. Paucimannose, hybrid, and complex mono-antennary classes were detected with relative intensities less than 1%.

To identify glycan structures specific to SCD, we compared the SCD RBC *N*-glycome to that of healthy donors (supplemental Table 4). Of the quantified glycan structures, 14 (12%) were significantly different ($P < .05$ and greater than twofold difference in

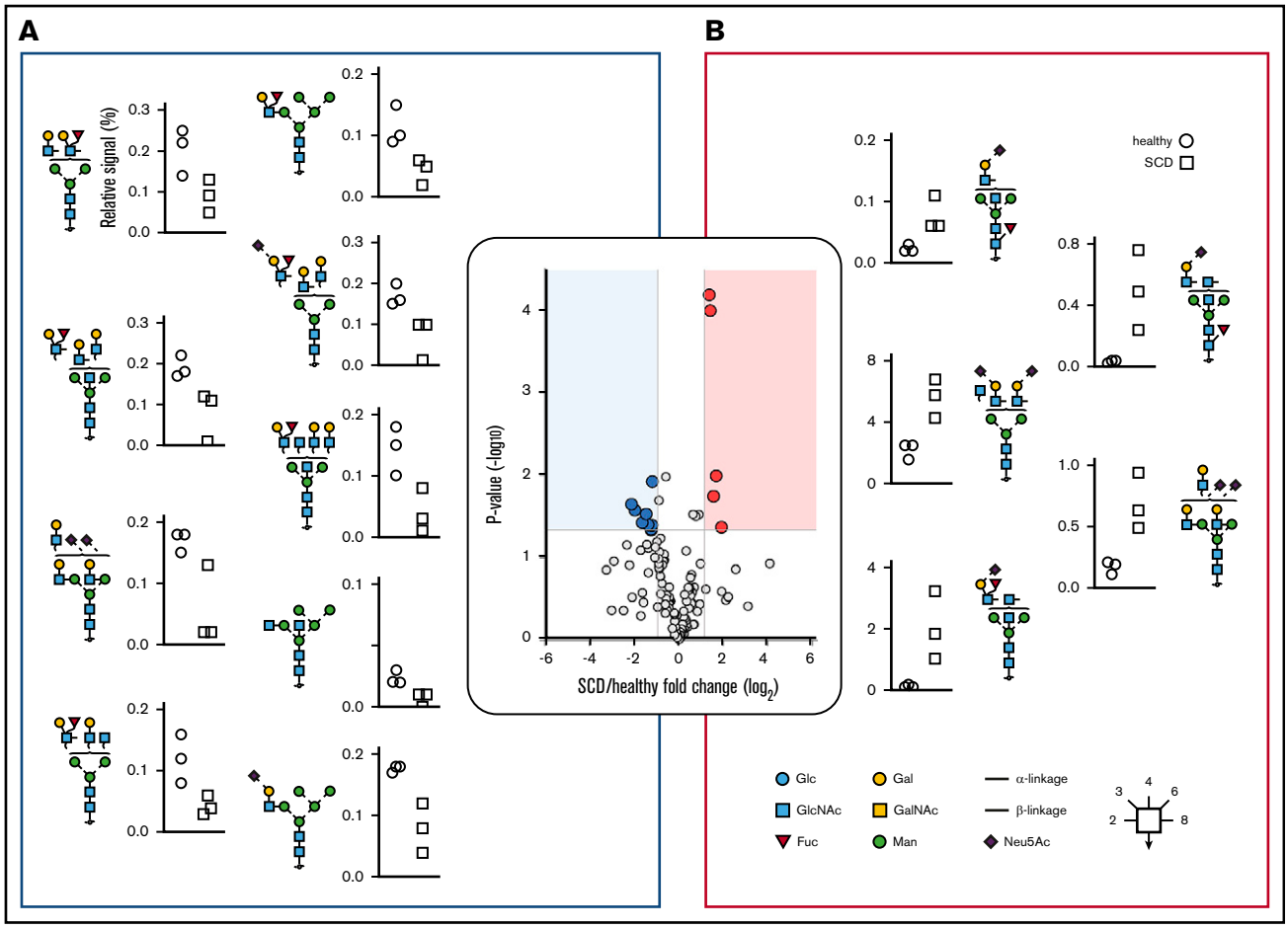

Figure 2. Mass spectrometry comparison of RBC *N*-glycans from healthy and SCD patients. Volcano plot of quantified RBC *N*-glycans with thresholds (shading) applied for significance ($P \leq .05$) and fold change (at least twofold) between control (n = 3) and SCD donors (n = 3). Colored data points are glycans selected for display left and right from the plot. (A) *N*-glycan structures that are significantly increased in healthy patients. (B) *N*-glycan structures that are significantly increased in SCD.

sickle cell/healthy average signal; Figure 2) between SCD and healthy samples. Five glycans had a higher signal in SCD samples, with all structures modified with α2,6 SA (ranging from 2.5- to 18-fold differences; Figure 2). Of the 9 glycans with higher signals in healthy donors, 3 structures are classed as hybrid-type glycans (two- to fourfold differences), and 3e structures were confirmed to feature α2,3 SA (two- to threefold differences; Figure 2). *O*-glycans were similarly analyzed, but no significant differences were detected between healthy and SCD RBCs (supplemental Table 5). These results agree with those observed by lectin array, as increases in SSA and SNA binding denote increases in α2,6 SA. Conversely, mass spectrometry analysis points to a decrease in α2,3 SA in SCD compared with healthy donors, supporting the increased terminal galactose moieties identified by lectins.

Glycan microarrays identify increased binding of proteins in SCD plasma to immunogenic mucin-associated structures

As changes in glycan expression in RBCs between healthy donors, SCT donors, and SCD samples were identified, we hypothesized that these glycan changes would translate to downstream alterations of plasma GBPs. To determine differences in GBP binding between healthy and SCD samples, we applied plasma to a 100-glycan microarray (Figure 3A) featuring a broad array of blood group and Lewis antigens, milk oligosaccharides, gangliosides and glycosaminoglycans, and globo-series glycolipids. These broad glycan motifs can serve as a screening tool for GBPs, including antibodies formed during immune responses.

Samples were well separated based on disease state using sPLS-DA (Figure 3B). Moderated *t* tests of normalized data showed significant changes in glycan binding between healthy and SCD samples and SCT and SCD samples ($P \leq .05$; for glycan structure numbers and identification, see supplemental Table 7).

Increased GBP binding to fucosylated glycan motifs in SCD was observed, including 3-sialyl-3-fucosyllactose (F-SL), Lewis Y, terminal Lewis A, and Gal-β-1,4-(Fuc-α-1,3)-GlcNAc-β-1,3-Gal-β) (glycans #64, 71, 73 and 63, respectively). GBP binding to asialo, α2,6-sialylated and di-sialylated (Neu5Ac-α-2,6-[Neu5Ac-α-2,3]-Gal-β-1,3-GalNAc-β) core-1 *O*-glycan structures (glycans 22, 44, and 48, respectively) was also increased in SCD samples. Additionally, GBP binding to chitin-trisaccharide and isomaltose was increased in SCD plasma, suggesting increased antimicrobial immune responses. GBP binding to glycans 39 (Neu5Ac-α-2,6-Gal-β-1,4-Glc-β), 74 (Gal-α-1,3-Gal-β-1,3-GlcNAc-β), and 26

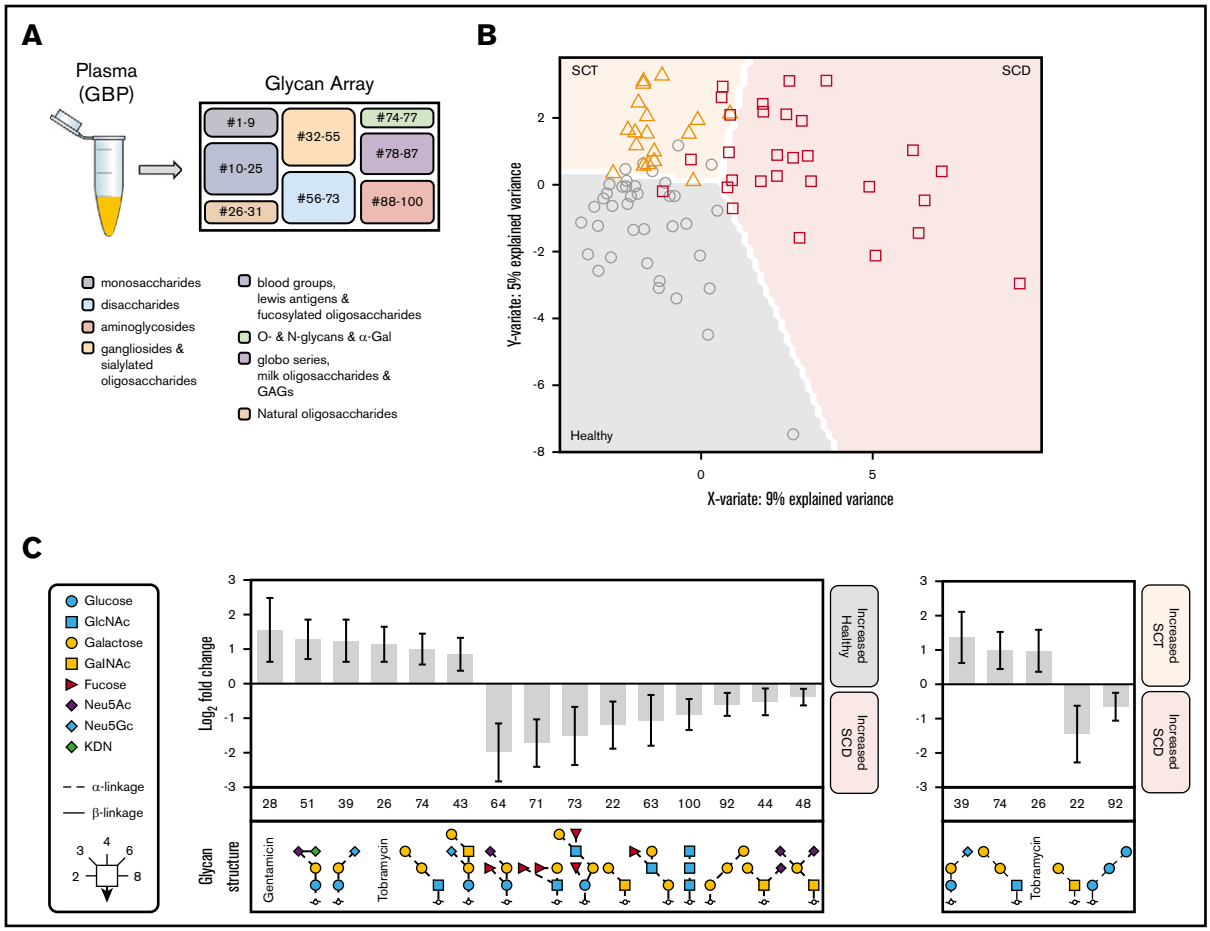

Figure 3. Changes in glycan binding observed among healthy, SCT, and SCD plasma samples using glycan microarrays. (A) GBP binding to 100 different glycan structures was measured using Glycan Array (RayBiotech). Glycans are split into structural/functional groups based on numbering. (B) Data obtained from healthy, SCD, and SCT patients were normalized using a quantile method and analyzed using a sparse partial least squares discriminant analysis (sPLS-DA) method. All glycan structures are listed with numerical classification in supplemental Figure 2 with additional contributing glycans to component 1 and 2 of separation shown in supplemental Figure 3. The receiver operating characteristic values are as follows: healthy vs others = 0.827; SCT vs others = 0.6526; SCD vs others = 0.9729. (C) Data showed significant differences in SCD compared with healthy and SCT groups ($P \leq .05$) with $\log_2$ fold changes between 2 and −2 (95% CI bars shown; for full *t* test results, see supplemental Table 7). Glycan structures for each numerical classification are shown with linkage information. Disease state preferences for each glycan are also indicated. Glycan names can be found in supplemental Table 6.

(tobramycin) (Figure 3C) was decreased in SCD plasma. The data show that SCD patients have increased GBPs to immunogenic mucin glycan motifs (Lewis A and Y, and asialo and α2,6-sialylated core 1 structures) often associated with cancer and chronic inflammation and suggests a heightened immune response to aberrant glycosylation.

MixOmics affirms aberrant RBC glycans and GBP binding in SCD but additionally reveals changes in ABO blood group expression and extra GBP binding targets

To combine the analysis of our different data sets, we used MixOmics (DIABLO),[51] an R package that uses a multivariate method for integration of biological datasets with a particular focus on variable selection measured on the same biological samples.[50,51] MixOmics analysis distinguished healthy and SCD samples based on a unique combination of glycans and lectins (Figure 4) but was not able to isolate SCT samples. Changes in glycan and lectin binding observed with individual analyses were reaffirmed in the integrated MixOmics analysis with the addition of new interarray associations missed by singular analysis. The combined heat map showed (1) higher fluorescence in 8 lectins and 13 glycans and (2) lower fluorescence in 8 lectins and 8 glycans in SCD patients.

Sialyation changes were again observed with increased α2,6 sialylation (SSA, SNA) and decreased α2,3 sialyation (WGA, MAH) on RBCs, distinguishing SCD patients from healthy donors. However, new increased GPB binding to an α2,8 SA baring oligosaccharide (Neu5Ac-α-2,8-Neu5Ac-α-2,6-Gal-β-1,4-Glc, 54), attributed to chronic inflammation,[22] was also detected by MixOmics.

Group O and A individuals display Fucα1-2Galβ1-4GlcNAc and GalNAcα1-3(Fucα1-2)Galβ1-4GlcNAc glycan structures, respectively.[55] The RBC i/I blood group system is represented by unbranched and branched polylactosamine glycans, respectively.[56-58] Lectins able to distinguish blood group related antigens including LTL (group O)

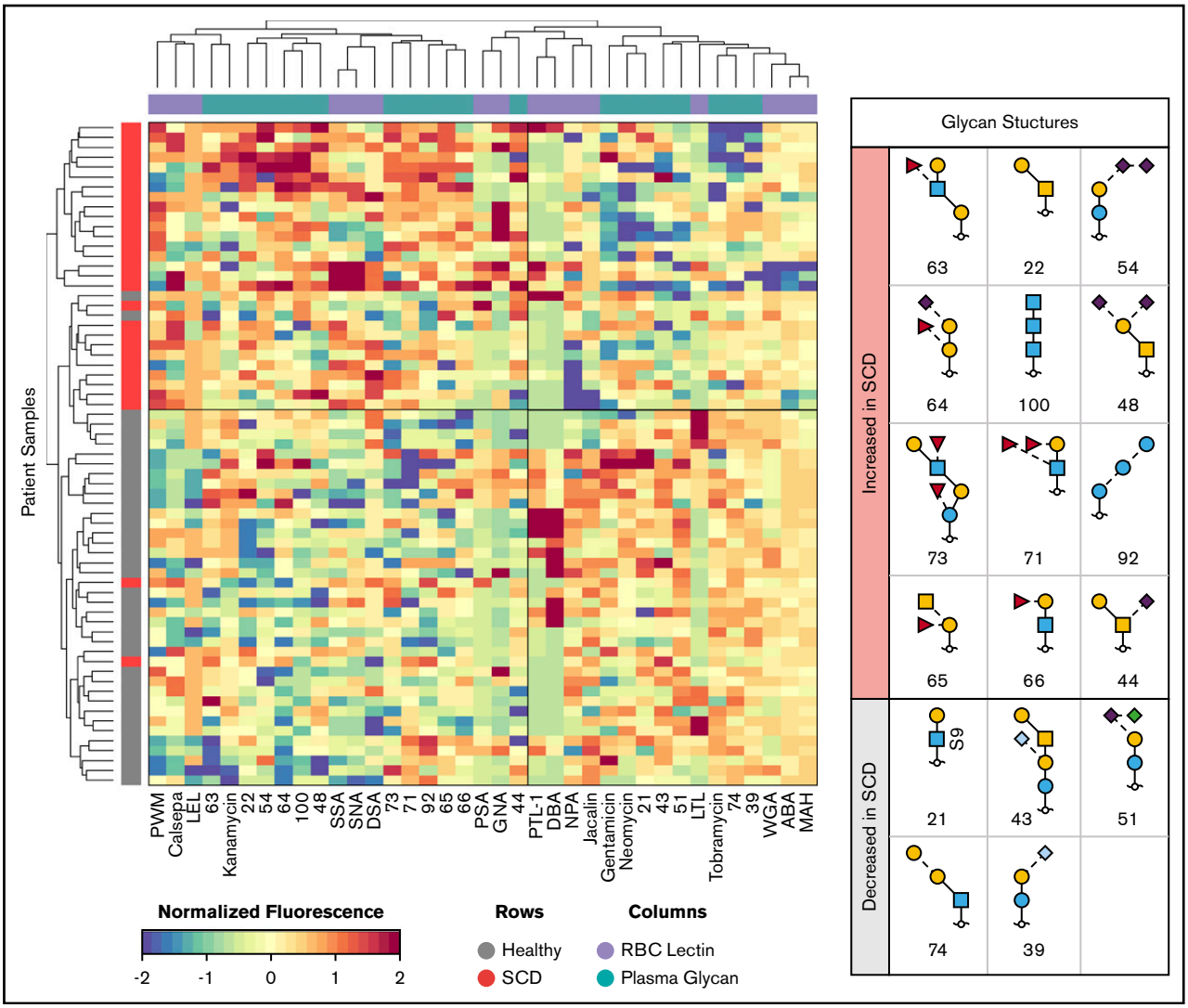

Figure 4. Correlation of healthy and SCD samples between lectin and glycan arrays determined using predictive learning processes. Heat map of specific lectins and glycans responsible for statistic separation of healthy and SCD samples. Approximate quadrants are boxed where there is a noticeable trend in expression levels. Corresponding glycan structures are displayed to the right.

and both DBA and PTL-I (group A) showed decreased recognition in SCD patients, but LEL and DSA (i/I blood group) were observed to increase binding, suggesting terminal blood group antigen alterations on RBCs in SCD. Notably, MixOmics detected new increases in GBP binding to blood group A and H antigens (65 and 66) in SCD, with a reciprocal decrease of group A– and O–specific lectin binding (LTL and DBA) to RBCs. Additionally, decreased GBP binding to a sulfated lactosamine structure (Gal-β-1,4-(6S)GlcNAc-β, #21) was detected, further reinforcing the notion that blood group antigen expression differs in SCD. Using MixOmics we also observed increases of PWM and GNA binding and decreases of NPA binding to SCD RBCs, suggesting alterations in mannose moieties, and decreased binding of Galactose and GalNAc recognizing lectins (ABA, Jacalin).

GBPs showed increased recognition of immunogenic mucin-associated glycans in SCD, including Lewis Y, Lewis A, asialo, α2,6-sialylated and di-sialylated core 1 structures (glycans 71, 73, 22, 44, 48). GBPs binding to other fucosylated oligosaccharides (Gal-β-1,4-[Fuc-α-1,3]-GlcNAc-β-1,3-Gal-β and F-SL) was also increased. Decreased binding to aminoglycoside antibiotics (18, gentamicin; 26, tobramycin; 31, neomycin) was measured, except for kanamycin (29), which may have shown an overall increase because of heavily increased fluorescence from a subset of 6 SCD patients.

MixOmics analysis reiterated our findings obtained using sPLS-DA and regular *t* test methods, reinforcing observations of changes in (1) blood group expression and antibodies directed to blood group antigens and (2) binding of GBPs to immunogenic mucin-associated glycans, including sialyl core 1, Lewis A and Y structures, and sialylation in SCD often associated with chronic inflammation and cancer.

Discussion

Previous SCD research has mainly focused on differences in receptor binding to RBCs and plasma components brought on by

changes in glycosylation.[22,59,60] However, little research has been performed to identify the structural glycosylation changes on RBCs and in plasma. Using a unique approach of pairing lectin and glycan microarrays with mass spectrometry to analyze healthy, SCT, and SCD plasma and RBCs, we found significant changes in both glycosylation of red cells, and glycan recognition of plasma GBPs between healthy and SCD samples.

Typically, RBCs in SCD have altered surface sialylation,[25] displaying an uneven distribution of SA compared with healthy cells.[61] We found consistent changes in sialylation between healthy and SCD RBCs using both lectin array and mass spectrometry. All structures that were significantly increased in SCD samples contained α2,6-Neu5Ac, consistent with increases in SSA and SNA lectin binding. Mass spectrometry data suggest that α2,6-Neu5Ac is either replacing α2,3-Neu5Ac structures or being added to terminal galactose observed on healthy RBCs. One reason for changes in surface SA could be because of differences in the age of circulating RBCs. Aging RBCs see reductions of surface sialylation between 10% and 30%,[61-64] and in some hemolytic anemias, decreases of surface SA by 50% have been observed after release of RBCs into circulation.[65]

Sickled RBCs are more susceptible to endothelial adhesion because of these changes in terminal SA, leading to vaso-occlusive episodes.[66,67] E- and P-selectins are expressed on activated endothelium and platelets.[22] Sialyl-Lewis X binds selectins and promotes leukocyte trafficking to lymph nodes and sites of inflammation.[19,20] In addition to SA modifications, selectin binding depends on fucose and sulfated glycan decorations.[59,60] Fucosylated glycans adorned the top 5 structures for which GBPs in SCD had higher affinity, including the immunogenic Lewis Y and Lewis A, suggesting that fucosylated structures and reciprocal GBPs are generated in SCD. Increased fucosylation is also observed in inflammatory conditions,[21,68] such as fucosylated IgG in rheumatoid arthritis.[69,70] Thus, changes in sialylation and fucose-containing structures on sickled RBCs could alter selectin and RBC–ligand interactions to drive inflammation in SCD.

Overexpression of sialyl Lewis Y and sialyl Lewis A is also associated with cancers and chronic inflammation. In support of a heightened immune response to aberrant glycans, GBP binding to asialo and sialyl core 1 structures (glycans 22, 44, and 48; Figure 3C) was increased in SCD, with these glycans often expressed on mucin-rich glycoproteins, including CD59, that help to signal RBC hemolysis.[71] Sickling of RBCs could increase the expression of aberrant glycans resulting in lysis.[72] A recent report shows that cholesterol-dependent lysins (intermedilysin) bind to sialyl-core 1 *O*-glycans using CD59 to promote RBC lysis,[73] further supporting the role of *O*-glycans in RBC destruction. The role of RBC glycolipid expression of antigenic glycan structures needs to be elucidated. However, our data highlight mucin *O*-glycans as potential therapeutic targets in SCD.

A limitation of our results is that, although SCD samples were collected before transfusion, it is impossible to discern transfused from endogenous patient RBCs because of repeat transfusions. Transfusions can be episodic or timed, ranging from every other week to monthly, therefore, based on an RBC lifetime of ~120 days, contributing significantly to the data acquired. Another limitation is that we cannot correlate our results to patient treatment regimes.

MixOmics analysis confirmed trends we observed with the lectin and glycan arrays individually. However, it also brought to light subtle blood group changes. Lectins known to bind both group O and A antigens (LTL, DBA, and PTL-I) showed decreased affinity to SCD RBCs, whereas those lectins with affinity for i/I blood group antigens (LEL and DSA) showed increased binding. The i blood group antigen is converted to I antigen within 18 months of birth, and therefore an increased binding of lectins to i/I antigens suggests more immature RBCs in SCD, which lack ABO antigens and the complete conversion of i to I antigens.[74] Previous studies have observed that RBC maturation in individuals with hemoglobinopathies decreases from 3 to 1.5 days with increased reactivity to i antibodies.[75] Additionally, increased erythropoiesis, as in SCD and thalassemia, can weaken the expression of ABO blood group antigens.[76,77] Loss of ABO antigens is also seen on the RBCs of myeloid malignancies[78] and on carcinoma tumor cells, suggesting that ABO antigen expression change contributes to the immune response in disease,[79-81] including SCD. Because of sample size limitations, only blood groups A and O were analyzed. Further investigation is needed to understand the impact of SCD on blood group expression.

In conclusion, our multipronged approach shows changes to both glycosylation on RBCs and binding of plasma proteins to aberrant glycans in SCD. Specifically, our data showed loss of α2,3-Neu5Ac and surprisingly revealed a reciprocal increase of α2,6-Neu5Ac on SCD RBCs, in addition to changes in blood group antigen expression consistent with more immature RBCs. Our data further show increased binding of plasma GBPs to potentially immunogenic glycans, including mucin core 1 and Lewis A and Lewis Y structures, suggesting these glycan structures as potential therapeutic targets.

Acknowledgments

This work was supported by National Institutes of Health, National Heart, Lung, and Blood Institute grants R01-HL126785 and R01-HL134010 (R.L.G.) and K12-HL141954 and R01-HL089224 (K.M.H.) and The Jacquelyn & Arlyn Fredrick Endowment Fund for Clinical Research (W.Q.A.). The Core Labs at the Blood Research Institute and the Medical College of Wisconsin Genomic Sciences and Precision Medicine Center and Mass Spectrometry Center provided key resources.

Authorship

Contribution: H.E.A. performed research, collected, analyzed, and interpreted results, and cowrote the manuscript; C.A. performed all mass spectrometry research, analyzed and interpreted the resulting data, and cowrote the manuscript; A.P.S. helped to collect results; R.L.G. helped to fund the research; K.M.H. helped to design the study and analyzed and interpreted results; W.Q.A. designed and helped perform research for the study and performed computational biological analysis; and all authors read, contributed to, and approved the writing of the manuscript.

Conflict-of-interest disclosure: The authors declare no competing financial interests.

ORCID profiles: H.E.A., 0000-0001-9722-629X; C.A., 0000-0001-5944-6179; R.L.G., 0000-0002-9263-833X; K.M.H., 0000-0001-6526-7919; W.Q.A., 0000-0003-2715-642X.

Correspondence: Karin M. Hoffmeister, Versiti Blood Research Institute, 8727 W Watertown Plank Rd, Milwaukee, WI 53226; e-mail: khoffmeister@versiti.org.

References

1. Strouse J. Sickle cell disease. *Handb Clin Neurol*. 2016;138:311-324.
2. Kato GJ, Piel FB, Reid CD, et al. Sickle cell disease. *Nat Rev Dis Primers*. 2018;4(1):18010.
3. Carden MA, Little J. Emerging disease-modifying therapies for sickle cell disease. *Haematologica*. 2019;104(9):1710-1719.
4. Moerdler S, Manwani D. New insights into the pathophysiology and development of novel therapies for sickle cell disease. *Hematology Am Soc Hematol Educ Program*. 2018;2018:493-506.
5. Telen MJ, Malik P, Vercellotti GM. Therapeutic strategies for sickle cell disease: towards a multi-agent approach. *Nat Rev Drug Discov*. 2019;18(2):139-158.
6. Agrawal RK, Patel RK, Shah V, Nainiwal L, Trivedi B. Hydroxyurea in sickle cell disease: drug review. *Indian J Hematol Blood Transfus*. 2014;30(2):91-96.
7. Orkin SH, Bauer DE. Emerging Genetic Therapy for Sickle Cell Disease. *Annu Rev Med*. 2019;70(1):257-271.
8. Kassim AA, Sharma D. Hematopoietic stem cell transplantation for sickle cell disease: The changing landscape. *Hematol Oncol Stem Cell Ther*. 2017;10(4):259-266.
9. Chen G, Chang J, Zhang D, Pinho S, Jang JE, Frenette PS. Targeting Mac-1-mediated leukocyte-RBC interactions uncouples the benefits for acute vaso-occlusion and chronic organ damage. *Exp Hematol*. 2016;44(10):940-946.
10. Telen MJ. Cellular adhesion and the endothelium: E-selectin, L-selectin, and pan-selectin inhibitors. *Hematol Oncol Clin North Am*. 2014;28(2):341-354.
11. Koehl B, Nivoit P, El Nemer W, et al. The endothelin B receptor plays a crucial role in the adhesion of neutrophils to the endothelium in sickle cell disease. *Haematologica*. 2017;102(7):1161-1172.
12. Wun T, Styles L, DeCastro L, et al. Phase 1 study of the E-selectin inhibitor GMI 1070 in patients with sickle cell anemia [published correction in *PLos One*. 2014;9(10):e111690]. *PLoS One*. 2014;9(7):e101301.
13. Telen MJ, Wun T, McCavit TL, et al. Randomized phase 2 study of GMI-1070 in SCD: reduction in time to resolution of vaso-occlusive events and decreased opioid use. *Blood*. 2015;125(17):2656-2664.
14. Varki A. Nothing in glycobiology makes sense, except in the light of evolution. *Cell*. 2006;126(5):841-845.
15. Schnaar RL. Glycobiology simplified: diverse roles of glycan recognition in inflammation. *J Leukoc Biol*. 2016;99(6):825-838.
16. Varki A. *Essentials of Glycobiology*. 3rd ed. Cold Spring Harbor, New York: Cold Spring Harbor Laboratory Press; 2017.
17. Müller J, Nitschke L. The role of CD22 and Siglec-G in B-cell tolerance and autoimmune disease. *Nat Rev Rheumatol*. 2014;10(7):422-428.
18. Macauley MS, Paulson JC. Siglecs induce tolerance to cell surface antigens by BIM-dependent deletion of the antigen-reactive B cells. *J Immunol*. 2014;193(9):4312-4321.
19. Borsig L. Selectins in cancer immunity. *Glycobiology*. 2017;28(9):648-655.
20. Winkler IG, Barbier V, Nowlan B, et al. Vascular niche E-selectin regulates hematopoietic stem cell dormancy, self renewal and chemoresistance. *Nat Med*. 2012;18(11):1651-1657.
21. Becker DJ, Lowe JB. Fucose: biosynthesis and biological function in mammals. *Glycobiology*. 2003;13(7):41R-53R.
22. Varki A. Sialic acids in human health and disease. *Trends Mol Med*. 2008;14(8):351-360.
23. Ekeke GI, Ibeh GO. Sialic acid in sickle cell disease. *Clin Chem*. 1988;34(7):1443-1446.
24. Onyemelukwe GC, Esievo KA, Kwanashie CN, Kulkarni AG, Obinechie EN. Erythrocyte sialic acid in human sickle-cell disease. *J Comp Pathol*. 1987;97(2):143-147.
25. Kiser ZM, Lizcano A, Nguyen J, et al. Decreased erythrocyte binding of Siglec-9 increases neutrophil activation in sickle cell disease. *Blood Cells Mol Dis*. 2020;81:102399.
26. Kucuk O, Gilman-Sachs A, Beaman K, Lis LJ, Westerman MP. Antiphospholipid antibodies in sickle cell disease. *Am J Hematol*. 1993;42(4):380-383.
27. Connor WE, Lin DS, Thomas G, Ey F, DeLoughery T, Zhu N. Abnormal phospholipid molecular species of erythrocytes in sickle cell anemia. *J Lipid Res*. 1997;38(12):2516-2528.
28. Liu SC, Derick LH, Zhai S, Palek J. Uncoupling of the spectrin-based skeleton from the lipid bilayer in sickled red cells. *Science*. 1991;252(5005):574-576.
29. Galili U. Discovery of the natural anti-Gal antibody and its past and future relevance to medicine. *Xenotransplantation*. 2013;20(3):138-147.
30. Zhang D, Xu C, Manwani D, Frenette PS. Neutrophils, platelets, and inflammatory pathways at the nexus of sickle cell disease pathophysiology. *Blood*. 2016;127(7):801-809.
31. Sparkenbaugh E, Pawlinski R. Prothrombotic aspects of sickle cell disease. *J Thromb Haemost*. 2017;15(7):1307-1316.
32. Muthana SM, Gildersleeve JC. Factors affecting anti-glycan IgG and IgM repertoires in human serum. *Sci Rep*. 2016;6(1):19509.
33. Anani WQ, Ashwood HE, Schmidt A, Burns RT, Denomme GA, Hoffmeister KM. Predictive modeling of complex ABO glycan phenotypes by lectin microarrays. *Blood Adv*. 2020;4(16):3960-3970.
34. Boyum A. Separation of lymphocytes, lymphocyte subgroups and monocytes: a review. *Lymphology*. 1977;10(2):71-76.

35. Heinrich V, Ritchie K, Mohandas N, Evans E. Elastic thickness compressibilty of the red cell membrane. *Biophys J*. 2001;81(3):1452-1463.

36. Dodge JT, Mitchell C, Hanahan DJ. The preparation and chemical characteristics of hemoglobin-free ghosts of human erythrocytes. *Arch Biochem Biophys*. 1963;100(1):119-130.

37. Ashwood C, Waas M, Weerasekera R, Gundry RL. Reference glycan structure libraries of primary human cardiomyocytes and pluripotent stem cell-derived cardiomyocytes reveal cell-type and culture stage-specific glycan phenotypes. *J Mol Cell Cardiol*. 2020;139:33-46.

38. Jensen PH, Karlsson NG, Kolarich D, Packer NH. Structural analysis of N- and O-glycans released from glycoproteins. *Nat Protoc*. 2012;7(7):1299-1310.

39. Ashwood C, Pratt B, MacLean BX, Gundry RL, Packer NH. Standardization of PGC-LC-MS-based glycomics for sample specific glycotyping. *Analyst (Lond)*. 2019;144(11):3601-3612.

40. Kessner D, Chambers M, Burke R, Agus D, Mallick P. ProteoWizard: open source software for rapid proteomics tools development. *Bioinformatics*. 2008;24(21):2534-2536.

41. Cooper CA, Gasteiger E, Packer NH. GlycoMod—a software tool for determining glycosylation compositions from mass spectrometric data. *Proteomics*. 2001;1(2):340-349.

42. Ashwood C, Lin CH, Thaysen-Andersen M, Packer NH. Discrimination of isomers of released N- and O-glycans using diagnostic product ions in negative ion PGC-LC-ESI-MS/MS. *J Am Soc Mass Spectrom*. 2018;29(6):1194-1209.

43. MacLean B, Tomazela DM, Shulman N, et al. Skyline: an open source document editor for creating and analyzing targeted proteomics experiments. *Bioinformatics*. 2010;26(7):966-968.

44. Ceroni A, Maass K, Geyer H, Geyer R, Dell A, Haslam SM. GlycoWorkbench: a tool for the computer-assisted annotation of mass spectra of glycans. *J Proteome Res*. 2008;7(4):1650-1659.

45. Everest-Dass AV, Abrahams JL, Kolarich D, Packer NH, Campbell MP. Structural feature ions for distinguishing N- and O-linked glycan isomers by LC-ESI-IT MS/MS. *J Am Soc Mass Spectrom*. 2013;24(6):895-906.

46. Struwe WB, Agravat S, Aoki-Kinoshita KF, et al. The minimum information required for a glycomics experiment (MIRAGE) project: sample preparation guidelines for reliable reporting of glycomics datasets. *Glycobiology*. 2016;26(9):907-910.

47. Kolarich D, Rapp E, Struwe WB, et al. The minimum information required for a glycomics experiment (MIRAGE) project: improving the standards for reporting mass-spectrometry-based glycoanalytic data. *Mol Cell Proteomics*. 2013;12(4):991-995.

48. Rojas-Macias MA, Mariethoz J, Andersson P, et al. Towards a standardized bioinformatics infrastructure for N- and O-glycomics. *Nat Commun*. 2019;10(1):3275.

49. Sharma V, Eckels J, Schilling B, et al. Panorama Public: a public repository for quantitative data sets processed in Skyline. *Mol Cell Proteomics*. 2018;17(6):1239-1244.

50. Rohart F, Gautier B, Singh A, Lê Cao KA. mixOmics: an R package for 'omics feature selection and multiple data integration. *PLOS Comput Biol*. 2017;13(11):e1005752.

51. Singh A, Shannon CP, Gautier B, et al. DIABLO: an integrative approach for identifying key molecular drivers from multi-omics assays. *Bioinformatics*. 2019;35(17):3055-3062.

52. Lewis-Beck MS, Bryman A, Liao TF. *The SAGE Encyclopedia of Social Science Research Methods*. Thousand Oaks, CA: SAGE; 2004.

53. Hirabayashi J, Kuno A, Tateno H. Lectin-based structural glycomics: a practical approach to complex glycans. *Electrophoresis*. 2011;32(10):1118-1128.

54. Liang CH, Wu CY. Glycan array: a powerful tool for glycomics studies. *Expert Rev Proteomics*. 2009;6(6):631-645.

55. Daniels G, Reid ME. Blood groups: the past 50 years. *Transfusion*. 2010;50(2):281-289.

56. Hakomori S. Blood group ABH and Ii antigens of human erythrocytes: chemistry, polymorphism, and their developmental change. *Semin Hematol*. 1981;18(1):39-62.

57. Bierhuizen MF, Mattei MG, Fukuda M. Expression of the developmental I antigen by a cloned human cDNA encoding a member of a beta-1,6-N-acetylglucosaminyltransferase gene family. *Genes Dev*. 1993;7(3):468-478.

58. Marsh WL. Anti-i: a cold antibody defining the Ii relationship in human red cells. *Br J Haematol*. 1961;7(2):200-209.

59. Rosen SD. Ligands for L-selectin: homing, inflammation, and beyond. *Annu Rev Immunol*. 2004;22(1):129-156.

60. Ley K. The role of selectins in inflammation and disease. *Trends Mol Med*. 2003;9(6):263-268.

61. Kahane I, Polliack A, Rachmilewitz EA, Bayer EA, Skutelsky E. Distribution of sialic acids on the red blood cell membrane in beta thalassaemia. *Nature*. 1978;271(5646):674-675.

62. Jakubowska-Solarska B, Solski J. Sialic acids of young and old red blood cells in healthy subjects. *Med Sci Monit*. 2000;6(5):871-874.

63. Mehdi MM, Singh P, Rizvi SI. Erythrocyte sialic acid content during aging in humans: correlation with markers of oxidative stress. *Dis Markers*. 2012;32(3):179-186.

64. Huang YX, Wu ZJ, Mehrishi J, et al. Human red blood cell aging: correlative changes in surface charge and cell properties. *J Cell Mol Med*. 2011;15(12):2634-2642.

65. Rachmilewitz EA, Kahane I. The red blood cell membrane in thalassaemia. *Br J Haematol*. 1980;46(1):1-6.

66. Hebbel RP. Beyond hemoglobin polymerization: the red blood cell membrane and sickle disease pathophysiology. *Blood*. 1991;77(2):214-237.

67. Kaul DK, Fabry ME, Windisch P, Baez S, Nagel RL. Erythrocytes in sickle cell anemia are heterogeneous in their rheological and hemodynamic characteristics. *J Clin Invest*. 1983;72(1):22-31.

68. Freeze HH, Kinoshita T, Varki A. Glycans in acquired human diseases. In: Varki A, Cummings RD, Esko JD, et al, eds. *Essentials of Glycobiology*. Cold Spring Harbor, NY: Cold Spring Harbor Laboratory Press; 2015:583-595.

69. Flögel M, Lauc G, Gornik I, Macek B. Fucosylation and galactosylation of IgG heavy chains differ between acute and remission phases of juvenile chronic arthritis. *Clin Chem Lab Med*. 1998;36(2):99-102.

70. Gornik I, Maravić G, Dumić J, Flögel M, Lauc G. Fucosylation of IgG heavy chains is increased in rheumatoid arthritis. *Clin Biochem*. 1999;32(8):605-608.

71. Meletis J, Terpos E, Samarkos M, et al. Detection of CD55- and/or CD59-deficient red cell populations in patients with lymphoproliferative syndromes. *Hematol J*. 2001;2(1):33-37.

72. Ilesanmi OO. Pathological basis of symptoms and crises in sickle cell disorder: implications for counseling and psychotherapy. *Hematol Rep*. 2010;2(1):e2.

73. Shewell LK, Day CJ, Jen FE, et al. All major cholesterol-dependent cytolysins use glycans as cellular receptors. *Sci Adv*. 2020;6(21):eaaz4926.

74. Cooling L. An update on the I blood group system. *Immunohematology*. 2019;35(3):85-90.

75. Hillman RS, Giblett ER. Red cell membrane alteration associated with "marrow stress". *J Clin Invest*. 1965;44(10):1730-1736.

76. Dean L. ABO blood group. In: Pratt VM, McLeod HL, Rubinstein WS, et al, eds. *Medical Genetics Summaries*. Bethesda, MD: National Center for Biotechnology Information; 2012.

77. Giblett ER, Crookston MC. Agglutinability of red cells by anti-I in patients with thalassemia major and other haematological disorders. *Nature*. 1964;201(4924):1138-1139.

78. Bianco T, Farmer BJ, Sage RE, Dobrovic A. Loss of red cell A, B, and H antigens is frequent in myeloid malignancies. *Blood*. 2001;97(11):3633-3639.

79. Bryne M, Thrane PS, Dabelsteen E. Loss of expression of blood group antigen H is associated with cellular invasion and spread of oral squamous cell carcinomas. *Cancer*. 1991;67(3):613-618.

80. Lee JS, Ro JY, Sahin AA, et al. Expression of blood-group antigen A—a favorable prognostic factor in non-small-cell lung cancer. *N Engl J Med*. 1991;324(16):1084-1090.

81. Limas C, Lange P, Fraley EE, Vessella RLA. A, B, H antigens in transitional cell tumors of the urinary bladder: correlation with the clinical course. *Cancer*. 1979;44(6):2099-2107.